Folded free-space polarization-controlled multistage interconnection network

Dan M. Marom, Paul E. Shames, Fang Xu, and Yeshaiahu Fainman

We present a folded free-space polarization-controlled optical multistage interconnection network (MIN) based on a dilated bypass–exchange switch (DBS) design that uses compact polarization-selective diffractive optical elements (PDOE's). The folded MIN design has several advantages over that of the traditional transparent MIN, including compactness, spatial filtering of unwanted higher-order diffraction terms leading to an improved signal-to-noise ratio (SNR), and ease of alignment. We experimentally characterize a folded 2×2 switch, as well as a 4×4 and an 8×8 folded MIN that we have designed and fabricated. We fabricated an array of off-axis Fresnel lenslet PDOE's with a 30:1 SNR and used it to construct a 2×2 DBS with a measured SNR of 60:1. Using this PDOE array in a 4×4 MIN resulted in an increased SNR of 120:1, highlighting the filtering effect of the folded design.

OCIS codes: 090.1760, 060.4250, 200.4650, 060.1810, 200.2610, 230.5440.

1. Introduction

As the demand for communication and computing services increases, there is a correlated growth in the need to switch among large numbers of input–output ports that carry high-bandwidth signals. Multistage interconnection networks (MIN's) are an attractive switching architecture because of the minimal number of switching elements required.[1] An optical MIN switching system routing high-bandwidth optical signals can play an important role in the development of ultrahigh-bandwidth interfaces with high-capacity parallel-access optical memories as well as for memory distribution. Various optical MIN system implementations have been reported, including guided-wave optics that use $LiNbO_3$ switches,[2] free-space optics with optoelectronic switches based on symmetrical self-electro-optic effect devices,[3] and transparent switches based on polarization modulators.[4–8] Transparent switches, in which an optical signal propagates without regeneration, do not introduce the additional limitations of optoelectronic device cost, speed, and power. Totally transparent systems depend on a centralized controller's performing the routing algorithm and serving user requests. Recently such a 4×4 free-space optical MIN based on polarization-selective diffractive optical elements (PDOE's) was demonstrated.[9] Optical MIN's have inherent insertion losses that can limit system scalability. However, attenuation can be compensated for by use of optical fiber amplifiers. Polarization-dependent systems can also take advantage of the recent advances in polarization-maintaining fibers or compensation in single-mode fibers.[10] Other performance metrics that can limit MIN scalability are optical cross talk, system compactness, system stability, and ease of alignment.

In this paper we describe the design and implementation of a free-space optical MIN by use of a novel folded dilated bypass–exchange switch (DBS) built of PDOE's that addresses these limitations. The use of a DBS allows for the elimination of the first-order cross talk that results from inaccuracies of polarization rotation[11] and diffractive optical element fabrication errors. By utilizing the three-dimensional functionality of the optical elements, one can then stack the DBS elements in the vertical dimension by folding (by use of a mirror plane) the switch along a central line of symmetry. The interconnection among multiple DBS's can also be folded, forming an optical MIN. This results in a resonator-type structure in which all the switching elements are distributed on a plane, providing a highly compact optical system that can easily be

The authors are with the Department of Electrical and Computer Engineering, University of California, San Diego, 9500 Gilman Drive, La Jolla, California 92093-0407.

Received 9 January 1998; revised manuscript received 1 June 1998.

0003-6935/98/296884-08$15.00/0

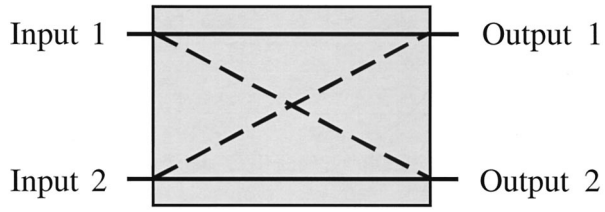

Fig. 1. BES functionality block diagram: solid lines, bypass mode in which the input to channel 1 goes to the output of channel 1; dashed lines, exchange mode in which the input to channel 1 goes to that output of channel 2 and vice versa.

aligned. Additionally, the use of space-variant diffractive optics permits the implementation of any interconnection topology corresponding to arbitrary network architectures. Finally, the use of micromirrors to fold the DBS allows for spatial filtering of the undesired diffraction orders, thereby decreasing the cross talk.

In Section 2 we review MIN switching concepts based on PDOE's. In Section 3 we introduce the folded implementation of the DBS by use of PDOE's. In Section 4 we discuss system design and component fabrication and characterization. Performance evaluation of a 2×2 folded DBS as well as multistage 4×4 and 8×8 folded optical MIN's is presented in Section 5. Finally, in Section 6 we summarize our research and discuss conclusions.

2. Free-Space Optical Multistage Interconnection Networks with Bypass–Exchange Switches

The basic structure of a MIN has alternating arrays of fixed interconnection patterns and switching modules, typically bypass–exchange switches (BES's). The MIN architecture determines the fixed interconnection pattern between switching stages and the number of stages implemented. Various MIN architectures are differentiated by the number of switching stages, complexity of routing algorithms, and network protocols. An optical MIN implemented with space-variant lenslets in free space permits the implementation of arbitrary network architectures and interconnection patterns. Here we demonstrate a folded 8×8 MIN based on a banyan architecture. However, the cross-talk and fabrication issues addressed also apply to any other architecture implementation.

The BES is a 2×2 switch with two allowed states: bypass, in which the signals of the two channels are unchanged (i.e., the input to channel 1 goes to the output of channel 1), and exchange, in which the signals go to the opposite output ports or channels (Fig. 1). Other possible states, known as broadcast and combine, are not considered in this application. A possible optical implementation of the BES uses the polarization state for switching. Two orthogonally polarized light beams are controlled by a polarization rotator to set the state of the switch and the polarization-selective optical elements (e.g., polarization beam-splitter cubes, birefringent crystals, and PDOE's) to direct the beams.

A birefringent computer-generated hologram[12] (BCGH) is an example of a compact and efficient PDOE. A BCGH element has an independent impulse response for each state of the two orthogonal linear polarizations, achieved by the etching of phase encodings into birefringent media. A compact 2×2 optical BES that uses BCGH elements has been demonstrated[8] (Fig. 2): The first BCGH element combines and focuses two inputs into the polarization rotator, which either exchanges their polarizations or does not. The second BCGH separates and directs the outputs to different destinations according to their polarization states.

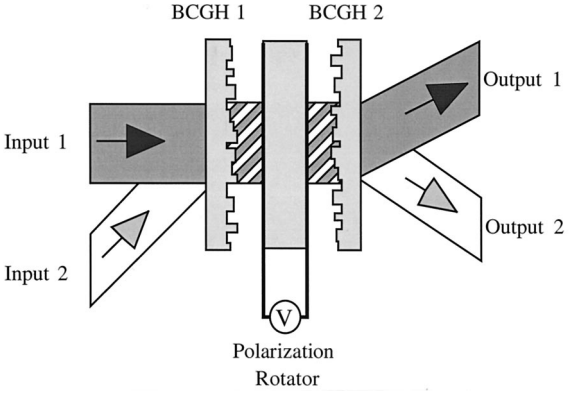

Fig. 2. Optical implementation of the BES: the first BCGH collimates the two input beams and the second BCGH directs the output beams depending on the polarization states. The voltage on the polarization rotator determines the state of the switch.

Inaccuracies of the polarization rotator and the BCGH fabrication can result in cross talk in this implementation of the BES. The polarization rotator can be characterized by an associated error of δ in the rotation angle, which results in a cross-talk term proportional to $\sin(|\delta|)$. The BCGH elements can be described by an associated cross talk ϵ that is due to fabrication errors such as etch depth and misalignment among multiple masks. The combined cross-talk component at the output of the BES is proportional to $|\delta| + |\epsilon|$, assuming that $\delta, \epsilon \ll 1$. The signal-to-noise ratio (SNR) of a MIN can be described by

$$\mathrm{SNR} = \log_{10}\left(\frac{1}{\delta_c}\right) - \log_{10} S, \tag{1}$$

where $\delta_c = |\delta| + |\epsilon|$ and S is the number of interconnection stages.[9] For increased scalability of the MIN network size (i.e., S is growing) the cross talk δ_c of each stage must be reduced, yielding the SNR necessary to support the desired bit-error rate.[13]

An improvement in cross-talk performance can be achieved by use of a DBS.[11] The DBS, which has two input and two output signals, comprises four 1×2 switches coupled together. The structure of the DBS guarantees that each 1×2 switch has only one signal propagating through it and that the majority of the cross-talk terms exit from the unutilized output ports. It can be shown that the remaining cross talk δ_c is now reduced to $\delta^2 + \epsilon^2$. Under the assumption

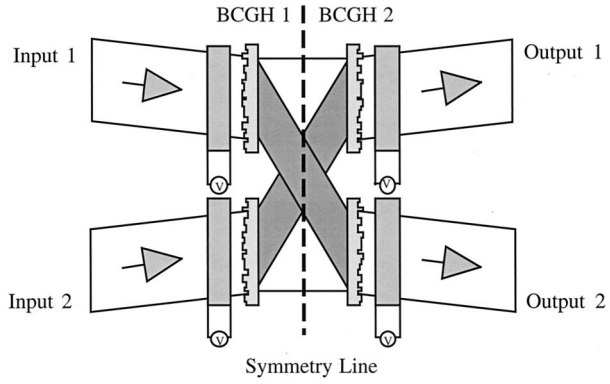

Fig. 3. Optical implementation of the DBS. Each BCGH element performs 1×2 switching, depending on the state of the polarization-rotator element. The input and the output states of the two channels are identical, permitting filtering with a polarizer of linear cross talk at the output.

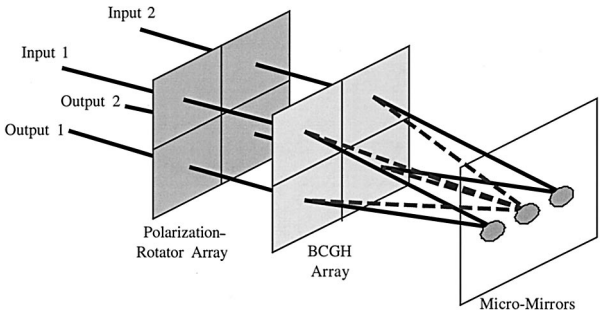

Fig. 4. Folded optical DBS. Similar elements (i.e., BCGH's, polarization rotators) are placed in two-dimensional arrays. Micromirrors reflect only the desired diffraction order and filter out the unwanted orders. The four polarization rotators are always in the same state and can be replaced by one larger-sized element.

that $\delta, \epsilon \ll 1$, this performance is a significant improvement over that of a conventional BES.

A free-space DBS can be implemented with a combination of four BCGH's and four polarization-rotator elements (Fig. 3). Depending on the state of the first set (i.e., the first elements in channels 1 and 2) of polarization rotators, the first set of BCGH elements defines the bypass or exchange functionality of the switch. The second set of BCGH lenslets directs the output beams to the next DBS array (for a multistage configuration), where the direction is dictated by the interconnection architecture that is being implemented. The second set of polarization rotators returns the output polarizations to their original input states.

Unlike in the BES, in a DBS the polarization state of each channel remains independent of the others. In our case we specify the input and the output beams to have identical polarization states. Therefore, by placing a polarizer at the output of the DBS, we can eliminate the linear cross talk. In this case the four polarization-rotator elements will always be in the same states, i.e., all ON or all OFF.

3. Folded Dilated Bypass–Exchange Switch and Optical Multistage Interconnection Network

The DBS's complexity, although it mitigates linear cross-talk problems, increases the number of components required for it to have the same functionality as the BES. However, one can reduce the complexity of these switches by taking advantage of the symmetry of the DBS (dashed line in Fig. 3) and the three-dimensional functionality of our free-space optical elements. One does this by introducing a propagation-direction component along the vertical axis, i.e., a small incidence angle, as well as by placing a mirror at the line of symmetry (Fig. 4). The input beams will pass through a rotator–BCGH combination at one elevation and react according to the encoded information at that location, switching information in the horizontal direction. On reflection from the mirror the beam passes through another BCGH–rotator combination but at a lower elevation (Fig. 4). By folding the switch in this manner, one locates similar elements (e.g., BCGH lenslets) in the same plane. Therefore a single DBS can be fabricated by use of a mirror and 2×2 arrays of BCGH's and polarization-rotator elements. The four polarization rotators, which are always in identical states, can be replaced with one larger polarization-rotator element. However, if we wish to consider other switching functionalities such as broadcast and combine states, the four polarization rotators have to be controlled separately.

The advantage of this folding technique is further enhanced when it is applied to an optical MIN. When a mirror is placed at the output of the first folded DBS, the beam will reflect back at a lower elevation and be coupled into subsequent DBS's located below the first. In this manner all similar elements of multiple DBS's can be combined into two-dimensional arrays, minimizing the number of components required for the entire MIN: a single BCGH array, a polarization-rotator array, and a pair of folding micromirror arrays. A folded optical MIN is packaged as a resonator in which each round trip represents a stage and all stages are stacked vertically (Fig. 5). An input signal beam enters the system at a small angle and reflects through a prescribed number of stages before exiting in the desired spatial output channel.

Implementation of a free-space optical MIN by use of this folding technique and BCGH space-variant lenslets presents several unique advantages:

(a) Arbitrary architecture: The use of space-variant lenslets in each polarization-selective element allows for the design of arbitrary connection patterns such that any multistage network topology can be implemented. In the folded optical MIN the number of channels and the interconnection architecture used dictate the size of the arrays but do not increase the number of components. For example, an 8×8 optical MIN architecture (of $\log_2 8 = 3$

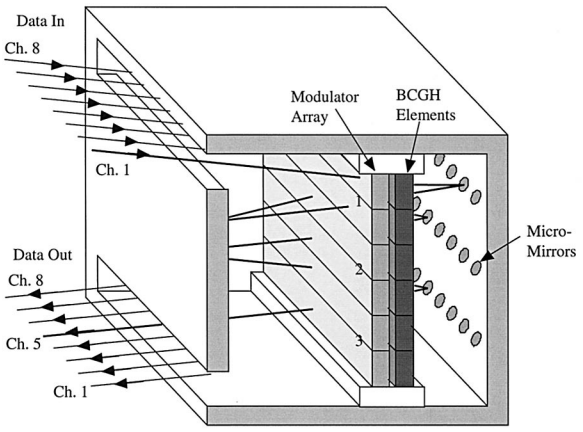

Fig. 5. Folded 8 × 8 optical MIN with one input beam, shown propagating from channel 1 to channel 5. In this example there are three stages of DBS's, which require three round-trip travels in the micromirror cavity.

stages) requires arrays of size 8 × 6 in BCGH's and polarization-rotator elements.

(b) Spatial filtering: A further advantage of the folded switch is that the mirror planes can also implement filtering functionality to increase SNR performance further. BCGH's are diffractive elements that, depending on the element design, can produce undesired diffraction terms. When continuous mirrors are used these undesired orders can propagate within the MIN, resulting in additional cross-talk noise at the output. However, if micromirrors deposited upon a transparent substrate are used, only the desired diffraction orders from the BCGH's will reflect back for further propagation, while the unwanted noise terms exit the system.

(c) Alignment: The arrangement of the optical elements in a two-dimensional array format also allows for relatively simple alignment of the system components. Correct alignment will dictate that the beams land on the correct elements during each pass through the cavity. The displacement of each beam from its correct position and the size of the beam at the BCGH elements (i.e., larger or smaller than the predicted size at the element) will indicate which optical elements (BCGH's, micromirrors, etc.) are incorrectly positioned. Inasmuch as the micromirror planes are mostly transparent, beam propagation within the cavity can be viewed with external imaging optics and a CCD camera. The beam size and position can therefore be monitored *in situ*, allowing for accurate alignment of optical elements and mirror planes.

4. System Design, Component Fabrication, and Their Characterization

To demonstrate a folded system, we designed and constructed an 8 × 8 optical MIN system (Fig. 6) based on a fully connected banyan architecture.[9] The design process of the system incorporates the following criteria: (i) maximization of the number of rings in off-axis Fresnel lenslets, (ii) minimum feature size of diffractive elements determined by the available fabrication technologies, and (iii) separation of diffractive-order beams at the micromirror plane. We developed a system-modeling tool by using Gaussian beam analysis of the stable mode of the micromirror-based (Fig. 5) cavity that calculates

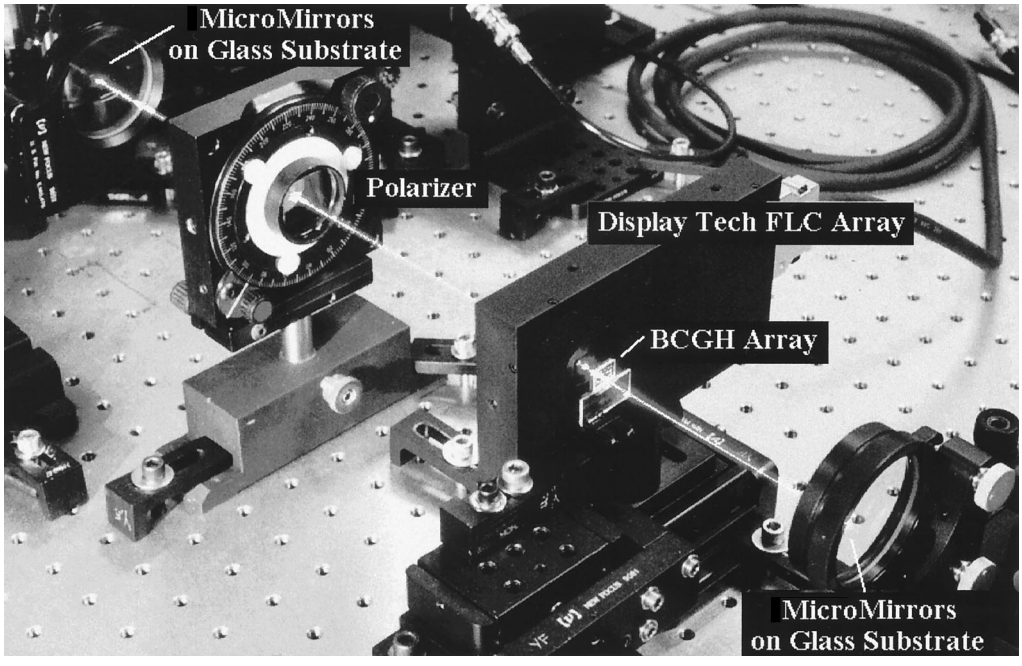

Fig. 6. Photograph of the experimental demonstration system of the folded optical MIN. The cavity is defined by two micromirror arrays deposited upon glass substrates. The polarizer is used to filter out the undesirable linear cross talk that is due to incorrect polarization rotation.

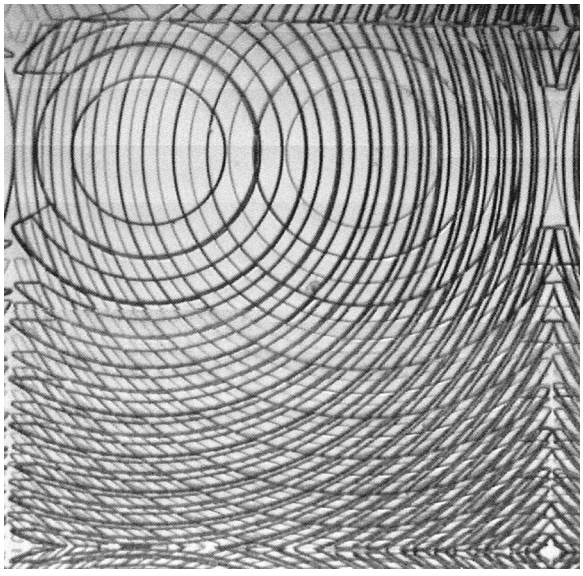

Fig. 7. CCD Image of a single BCGH element within an 8×6 array, showing multifunctional superposition of polarization-selective Fresnel lenslets.

these three parameters for a given cavity dimension. We found the optimal size of the cavity by varying the cavity dimensions over our design space and maximizing the above criteria.

The Gaussian beam spot size[14] at the BCGH lenslet plane was used as a limiting design constraint because at that location the beam size is largest. For a spot size greater than the lenslet (i.e., array pitch), optical power would leak into adjacent elements and give rise to cross talk. A spot size much smaller than the BCGH lenslet would result in a diminished diffraction efficiency. Our pitch size of 1 mm was determined by the dimensions of the pixel size of the polarization-rotator array used in our experiments. A beam spot size of 0.825 mm was used and provided minimal cross talk, high diffraction efficiency, and high power throughput (97% of the beam energy is contained in the 1 mm $\times$ 1 mm square). Accounting for beam propagation through multiple optical elements (BCGH, polarization rotator, etc.) yielded a lenslet focal length of 85.1 mm with a 300-μm waist size at one mirror plane and a 100-μm waist size at the other. The cavity length is 407 mm, with the BCGH element placed 107 mm from the back side mirror. The 1-mm pitch of the optical elements also dictates that the input light beam have an incidence angle of 0.4°. The polarization-rotator array is placed adjacent to the BCGH array to best match the 1-mm pitch of the ferroelectric liquid-crystal (FLC) elements.

Each of the designed BCGH lenslets functions as two independent off-axis Fresnel lenses for the two orthogonal polarization states (Fig. 7), whose offset is dictated by the deflection angle required by the interconnection pattern. The largest deflection angle for our 8×8 banyan network is 0.8°, corresponding to shifting the beam by 3 pixels. The BCGH was designed by use of the multiple-order delay approach[15] and fabricated in an YVO_4 crystal selected for its high value of birefringence. The advantages of using off-axis lenses include the following results: (i) The unwanted zero-order diffraction term can be filtered out of the cavity. Because the diffraction into the zero order is more sensitive to fabrication errors, which results in a strong unwanted residual component, we find that maximum extinction ratios can be attained by use of the first-order diffraction terms. (ii) The unwanted higher-order diffraction light is dispersed over a large area of the micromirror plane and is *not* focused onto the micromirrors [Fig. 8(a)]. The amount of optical power incident upon adjacent micromirrors (i.e., noise) and reflected back into the system is determined by the ratio of the area of the micromirror to the area of the diffracted order at the plane of the mirrors [Fig. 8(b)].

The measured first-order diffraction efficiencies of

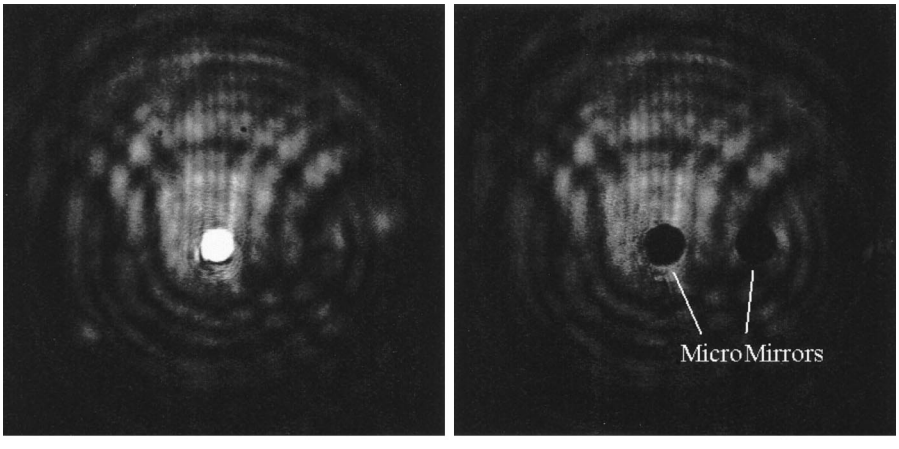

(a) (b)

Fig. 8. CCD pictures of (a) the output of one BCGH lenslet element for one polarization state, showing the focused first-order light and the unfocused higher diffraction orders, and (b) micromirrors (the dark circles), reflecting only first-diffraction-order light, permitting higher-diffraction-order light to exit the system.

the binary phase-level BCGH elements are 33% for vertical polarization and 35% for horizontal polarization, with extinction ratios better than 60:1. We also fabricated and tested four-phase-level BCGH diffractive elements, which require greater cumulative etch-depth errors because they have a more complicated fabrication process. These elements yielded 30:1 extinction ratios and diffraction efficiencies of 43% for vertical polarization and 46% for horizontal polarization. The relatively low extinction ratio and diffraction efficiency (compared with a theoretical efficiency of 80.5% for a four-phase-level diffractive optical element) is due primarily to etch-depth inconsistencies in the multistep fabrication process, which are described by the error term ϵ [see Eq. (1)].

The patterned arrays of micromirrors were etched onto a mirror fabricated by the evaporation of aluminum film onto optical flats, for which the average measured reflectance of the mirrors was 92%. The circular micromirrors have diameters of 400 and 150 μm, slightly larger than the calculated beam diameter at the mirror planes.

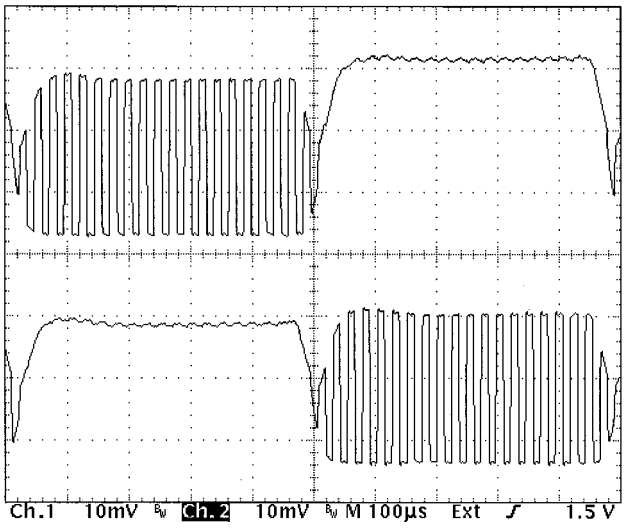

Fig. 9. Output signals for a single folded DBS (2×2 switch) with two input signals: a dc signal and a 20-kHz signal. The switch is reconfiguring at a 1-kHz rate, limited by the 100-μs characteristic rise time of the FLC. The measured average SNR is 57:1.

5. Multistage Interconnection Network System Experimental Characterization

Experimental testing of our 8×8 MIN system was performed with a 488-nm cw Gaussian beam generated by an argon laser. For initial testing we used two optical input channels, one with a dc signal and the other modulated by a NEOS Model N71003 acousto-optic (AO) cell. The polarization state of the beam as it propagates through the network is controlled by the two-dimensional array of FLC polarization rotators (DisplayTech, Model 10×10B). Reconfiguration of the FLC elements is under computer control, with a maximum switching speed (i.e., frame rate) of 0.2 ms. The output signals are measured by high-speed silicon p-i-n detectors.

For an 8×8 folded MIN the beam makes three round trips in the cavity (i.e., three layers of BES's). By diverting the beam after one or two passes, we are able to use the same experimental system to test the performance of a 2×2 (single DBS switch) or a 4×4 network. Using the binary phase-level BCGH elements, we measured the performance of a single DBS switch, which yielded extinction ratios of greater than 250:1. The extinction ratio for the DBS is significantly better (4:1) than those of the individual BCGH elements, which shows how the DBS eliminates significant cross talk. However, because of the low diffraction efficiency of the binary phase elements, the DBS switch has an insertion loss of approximately -11 dB and was not suitable for the multistage system experiments.

Figure 9 shows the output from a single DBS, constructed with the higher-efficiency four-phase-level BCGH, as it reconfigures between the bypass and the exchange modes at a 2-kHz rate (i.e., 500-μs packets). The AO signal is modulating one of the input signals with a square wave at 40 kHz (we used this relatively slow input signal to permit simultaneous oscilloscope visualization of both AO and FLC reconfiguration frequencies). The top and the bottom traces in Fig. 9 show the outputs of channel 1 and channel 2, respectively. Both configurations (i.e., bypass and exchange) produce extinction ratios (defined as the ratio between the ON state and the OFF state when one input signal is present) greater than 59:1 and a SNR (defined as the ratio of the signal to the noise at the same output, i.e., cross talk between two input signals) of greater than 57:1. Results of using signals ranging from dc to 10 MHz show similar SNR's, highlighting the optical transparency of the system. The extinction ratio improvement for the DBS is only 2:1 better than the extinction ratio of the diffraction orders of the four-phase-level elements used. This result is attributed to the much stronger cross talk that is due to fabrication errors (ϵ) seen in these elements. The higher diffraction efficiency of the four-phase-level BCGH reduced the insertion loss of the DBS to approximately -9 dB.

By allowing the beams to propagate two round trips through the cavity (by use of the four-phase-level BCGH elements), we experimentally characterized a multistage 4×4 system. Using a single dc input signal that switched among four output channels, we measured an average SNR of 90:1 and an extinction ratio of 120:1 (a 4:1 improvement over the individual BCGH elements). To investigate cross talk further, we introduced a second input signal. The measured output amplitudes are shown in Fig. 10. Most notable is that the output intensities vary depending on the output as well as the input channel, a result that might occur because of the variation of the lenslet diffraction efficiencies for different polarization states. The minimal average (i.e., the weakest output signal to the strongest output noise) SNR is 87:1.

The complete 8×8 interconnection system was

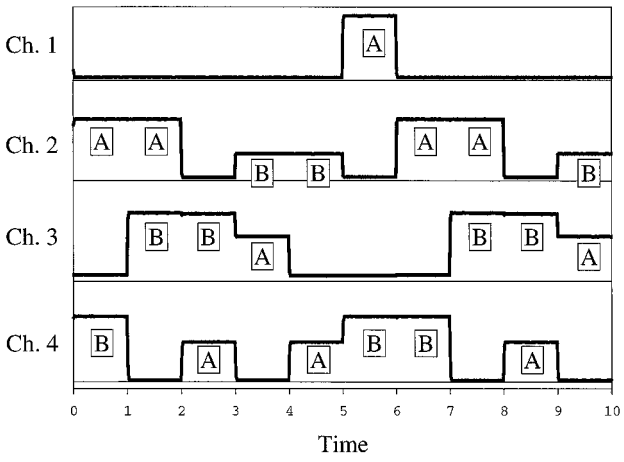

Fig. 10. Output from a 4 × 4 switch with two input signals (A and B) routed to the four output channels by a host computer controller. The average SNR is 120:1, which is twice as great as that of the single DBS performance, highlighting the filtering capabilities of the folded MIN configuration.

characterized with a single dc input signal that switched among all eight output channels. The output signals were relatively weak and were therefore imaged onto a CCD camera (which integrates over time) for detection (see Fig. 11). The average measured SNR was better than 30:1. This relatively low SNR can be attributed to the strong background noise and the small dynamic range of the CCD device used. We performed similar measurements by using two input signals that switched among all eight output channels that gave similar SNR results.

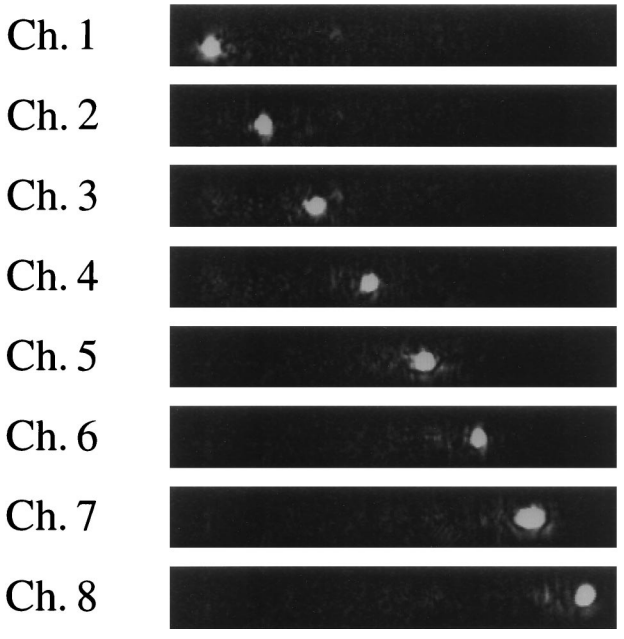

Fig. 11. CCD time-sequenced images showing a single input dc signal routing among eight output channels. The measured average SNR of 30:1 is derived from the CCD pixel values. This relatively low value might be due to the poor dynamic range and the background noise of the CCD device.

6. Discussion

We have described the design, fabrication, and testing of an optical MIN by using a novel folded architecture and compact polarization-selective BCGH elements. The design process determines the optimal system dimensions, which are constrained primarily by the limits of the diffractive optical fabrication facilities available. We have demonstrated how the folded design allows for the elimination of the first-order cross talk, ease of MIN system alignment and packageability, as well as filtering of unwanted high diffraction orders. The use of space-variant lenslets also allows for the implementation of arbitrary MIN architectures. The folded DBS (i.e., 2 × 2 switches) improved the extinction ratio compared with those of the single BCGH diffractive elements, binary and four-phase level, used. Further improvements in filtering out cross talk were seen in the 4 × 4 interconnection system, with measured extinction ratios of 120:1 (i.e., when input signals pass through two layers of DBS switches).

Traditional nonfolded MIN systems are planar by design and occupy an area proportional to their number of stages. However, such is not the case for our folded MIN, in which the stages are stacked vertically. The footprint that the system occupies depends on the length of the mirror cavity, which is dictated by the focal length and the deflection angle of the BCGH Fresnel lenslets. For off-axis lenslets the maximum deflection angle will be constrained by the minimum feature size of the fabrication process. However, for feature sizes smaller than five wavelengths,[16] the diffraction efficiency can be adversely affected.

When the N input channels are arranged in a $1 \times N$ vector form, the number of elements in the polarization rotator and BCGH arrays scales as N in the horizontal dimension and as $\log(N)$ in the vertical. As N increases, the ratio of the width to the height of the arrays is increased. For large N a relatively wide system can result, which will require relatively large deflection angles. An alternative strategy for maintaining system compactness is to arrange the N input channels in a rectangular array form (i.e., M rows of length N/M). This procedure would redistribute pixels from the same stage into multiple rows and would result in a more symmetric system that could significantly reduce the maximum degree of the deflection angles required.

The optical transparency of the MIN allows for transmission of very high data-rate signals. We tested our folded MIN with signals from dc to 10 MHz (the limit of our AO cell modulation speed) and found no change in the SNR or the extinction ratio. We expect system performance to be constant for signal bandwidths into the multigigahertz range. The limiting factor in interconnection reconfiguration is the rise and fall times of the employed FLC polarization-rotation elements. State-of-the-art FLC response times have approximately 10-μs rise times, but other

electro-optic materials could provide devices with orders-of-magnitude faster response times.[17]

The efficiency of the BCGH elements is the limiting factor in increasing the SNR of the multistage system. In our case the poor performance of the Fresnel lenslets can be attributed to two factors: (i) inaccurate etching depths owing to ion-etching device inconsistencies and (ii) use of the multiple-order delay approach to fabrication of BCGH elements, which has increased sensitivity to etch-depth errors. Significantly higher diffraction efficiencies can be expected with improved etching facilities and the use of other BCGH design approaches, such as dual-substrate[18] and form birefringent elements.[19]

The use of high-efficiency diffractive elements would also greatly reduce the insertion losses of these systems. For example, using 32-phase-level BCGH Fresnel lenslets with 97% diffraction efficiency[20] and dielectric mirrors with 99% reflectance as well as antireflectance coating of all optical surfaces would result in insertion losses less than −1 dB for each stage. For an interconnection system with 10 stages, which allows for 1024 input channels, the total insertion loss would be approximately −7 dB.

This research is funded in part by the National Science Foundation, the U.S. Air Force Office of Scientific Research, and the Rome Laboratory. Dan Marom acknowledges the support of the Fannie and John Hertz Foundation.

References

1. N. K. Ailiwadi, "Photonic switching architectures and their comparison," in *Frontiers of Computing Systems Research*, S. K. Tewksbury, ed. (Plenum, New York, 1990), Vol. 1, pp. 129–186.
2. T. Sawano, S. Suzuki, and M. Fujiwara, "A high-capacity photonic space-division switching system for broadband networks," J. Lightwave Technol. **13,** 335–340 (1995).
3. F. B. McCormick, T. J. Cloonan, F. A. P. Tooley, A. L. Lentine, J. M. Sasian, J. L. Brubaker, R. L. Morrison, S. L. Walker, R. J. Crisci, R. A. Novotny, S. J. Hinterlong, H. S. Hinton, and E. Kerbis, "Six-stage digital free-space optical switching network using symmetric self-electro-optic-effect devices," Appl. Opt. **32,** 5153–5171 (1993).
4. G. A. DeBiase, "Optical multistage interconnection networks for large-scale multiprocessor systems," Appl. Opt. **27,** 2017–2021 (1988).
5. K. M. Johnson, M. R. Surette, and J. Shamir, "Optical interconnection network using polarization-based ferroelectric liquid crystal gates," Appl. Opt. **27,** 1727–1733 (1988).
6. K. Noguchi, T. Sakano, and T. Matsumoto, "A rearrangeable multichannel free-space optical switch based on multistage network configuration," J. Lightwave Technol. **9,** 1726–1732 (1991).
7. D. M. Marom and D. Mendlovic, "Compact all-optical bypass–exchange switch," Appl. Opt. **35,** 248–253 (1996).
8. F. Xu, J. E. Ford, and Y. Fainman, "Polarization-selective computer-generated holograms: design, fabrication and applications," Appl. Opt. **34,** 256–266 (1995).
9. A. V. Krishnamoorthy, F. Xu, J. E. Ford, and Y. Fainman, "Polarization-controlled multistage switch based on polarization-selective computer-generated holograms," Appl. Opt. **36,** 997–1010 (1997).
10. F. Heismann, A. F. Ambrose, T. O. Murphy, and M. S. Whalen, "Polarization-independent photonic switching system using fast automatic polarization controllers," IEEE Photon. Technol. Lett. **5,** 1341–1343 (1993).
11. K. Padmanabhan and A. Netravali, "Dilated networks for photonic switching," IEEE Trans. Commun. **COM-35,** 1357–1365 (1987).
12. J. E. Ford, F. Xu, K. Urquhart, and Y. Fainman, "Polarization-selective computer-generated holograms," Opt. Lett. **18,** 456–458 (1993).
13. K. S. Urquhart, P. Marchand, Y. Fainman, and S. H. Lee, "Diffractive optics applied to free-space optical interconnects," Appl. Opt. **33,** 3670–3682 (1994).
14. A. Yariv, *Quantum Electronics* (Wiley, New York, 1989), Chap. 6.
15. F. Xu, R. C. Tyan, and Y. Fainman, "Single-substrate birefringent computer-generated holograms," Opt. Lett. **21,** 516–518 (1996).
16. D. A. Pommet, M. G. Moharam, and E. B. Grann, "Limits of scalar diffraction theory for diffractive phase elements," J. Opt. Soc. Am. A **11,** 1827–1834 (1994).
17. J. A. Thomas, M. Lasher, Y. Fainman, and P. Soltan, "A PLZT-based dynamic diffractive optical element for high speed random-access beam steering," in *Optical Scanning Systems: Design and Application*, L. Beiser and S. F. Sagan, eds., Proc. SPIE **3131,** 124–132 (1997).
18. N. Nieuborg, A. Kirk, B. Morlion, H. Thienpont, and I. Veretennicoff, "Polarization-selective diffractive optical elements with an index-matching gap material," Appl. Opt. **36,** 4681–4685 (1997).
19. F. Xu, R.-C. Tyan, P.-C. Sun, Y. Fainman, C.-C. Cheng, and A. Scherer, "Form birefringent computer-generated holograms," Opt. Lett. **21,** 1513–1515 (1996).
20. E. Pawlowski and B. Kuhlow, "Antireflection-coated diffractive optical elements fabricated by thin-film deposition," Opt. Eng. **33,** 3537–3546 (1994).